Resonant x-ray magnetic scattering at nonmagnetic ions

Michel van Veenendaal
Department of Physics, Northern Illinois University, De Kalb, Illinois 60115
and Argonne National Laboratory, 9700 South Cass Avenue, Argonne, Illinois 60439
(Received 6 February 2003; published 28 April 2003)

An explanation is given for the resonant x-ray magnetic scattering effects at the *K* edge of nonmagnetic ions observed by Mannix *et al.* [Phys. Rev. Lett. **86**, 4128 (2001)]. By using a description that goes beyond the usual fast-collision approximation, we can relate the scattering amplitude to the orbital moments on sites neighboring the nonmagnetic ion where the absorption takes place. The finite scattering amplitude is directly related to the resonant process, which explains the strong enhancement over the nonresonant intensity.

DOI: 10.1103/PhysRevB.67.134112 PACS number(s): 61.10.Dp, 78.70.Ck, 78.70.Dm

Resonant x-ray magnetic scattering (RXMS) and x-ray magnetic dichroism (XMD) are powerful tools for studying magnetic properties.[1–3] Integrated intensities of the spectra can be directly related to ground-state properties, such as $\langle L_z\rangle$ and $\langle S_z\rangle$.[4–6] These sum rules are commonly used for excitations into shells with well-established magnetic moments, such as the $3d$ and $4f$ shells of transition metals and rare earths, respectively. However, for excitations into other shells the situation is often more subtle. An example is the magnetic circular dichroism of the $5d$ band at the L edges of the rare earths.[7] Here the largest contribution to the XMD intensity is not the $5d$ magnetic moment, but the change in $2p\rightarrow 5d$ dipole matrix elements by the large $4f$ moment.

Even more surprising is the RXMS observed at the *K* edges of nonmagnetic anions, such as Ga in UGa_3 and As in UAs.[8] Here, there is no large moment on the ion that could explain the presence of a finite scattering amplitude. In addition to that, resonant enhancements of more than three orders of magnitude over the nonresonant intensity are observed. The most obvious explanation for these enhancements is a very small nonresonant scattering amplitude. Since this amplitude is proportional to $\mathbf{L}(\mathbf{k}_0-\mathbf{k}_f)\cdot\mathbf{A}+\mathbf{S}(\mathbf{k}_0-\mathbf{k}_f)\cdot\mathbf{B}$ where $\mathbf{A}$ and $\mathbf{B}$ are polarization vectors determined by $\mathbf{k}_0$, $\mathbf{e}_i$, $\mathbf{k}_f$, $\mathbf{e}_f$, and $\mathbf{L}$ and $\mathbf{S}$ are the Fourier transforms of the orbital and spin magnetization densities, respectively, a small scattering amplitude directly implies a small magnetic moment. However, since the standard RXMS sum rules[6] relate the scattering amplitude to $4p$ ground-state expectation values of L_z, this would immediately imply that also the resonant magnetic scattering amplitude is small. This is clearly in disagreement with the experimental data.

In this paper, we show that a finite scattering amplitude can still be obtained if we include the effects of the neighboring magnetic sites. By going beyond the commonly used fast-collision approximation,[6,9] we show that the excited electron probes the neighboring magnetic ions. This leads to a scattering operator for excitations at the *K* edge that can be expressed in ground-state expectation values of the nearest-neighbor orbital moments.

The intensity of RXMS in the dipole approximation I^1 is given by

$$I^1(\mathbf{e}_i,\mathbf{e}_f,\omega)=\left|\langle g|\mathbf{e}_f^*\cdot\mathbf{r}\frac{1}{\hbar\omega-H+i\Gamma/2}\mathbf{r}\cdot\mathbf{e}_i|g\rangle\right|^2, \quad (1)$$

where $\mathbf{e}_f$ and $\mathbf{e}_i$ are the initial and final polarization vectors of the light, respectively, $\hbar\omega$ is the photon energy, Γ is the lifetime broadening in the intermediate state, and H is the Hamiltonian of the system. In spherical coordinates, we can write the components of $\mathbf{r}$ as $r_\lambda=rC^1_\lambda(\hat{\mathbf{r}})$, where $\mathbf{C}^l(\hat{\mathbf{r}})$ is the renormalized spherical harmonic tensor with components $C^l_\lambda(\hat{\mathbf{r}})=\sqrt{4\pi/[l]}Y^l_\lambda(\hat{\mathbf{r}})$, with $[ll'\cdots]=(2l+1)(2l'+1)\cdots$. We can now write

$$I^1(\mathbf{e}_i,\mathbf{e}_f,\omega)=P^4_{1s,4p}|F^1(\mathbf{e}_i,\mathbf{e}_f,\omega)|^2, \quad (2)$$

where

$$P_{1s,4p}=\int_0^\infty r^2R_{1s}(r)R_{4p}(r)dr \quad (3)$$

gives the radial matrix element of the dipolar transition from the Ga or As *K* edge. The scattering amplitude F^1 can be written as

$$F^1(\mathbf{e}_1,\mathbf{e}_2,\omega)=\langle g|\mathbf{e}_2^*\cdot\mathbf{C}^{1*}(\hat{\mathbf{r}})G(\omega)\mathbf{C}^1(\hat{\mathbf{r}})\cdot\mathbf{e}_1|g\rangle, \quad (4)$$

where the Green's function is given by $G(\omega)=(\hbar\omega-H+i\Gamma/2)^{-1}$. Note that whereas RXMS is obtained from $|F^1(\mathbf{e}_i,\mathbf{e}_f,\omega)|^2$, the XMD spectrum is proportional to $\mathrm{Im}[F^1(\mathbf{e}_i,\mathbf{e}_i,\omega)]$, showing the intimate relation between XMD and RXMS.

It is common to recouple the scattering amplitude from Eq. (4) into a geometric and electronic part using

$$(\mathbf{a}^l\cdot\mathbf{b}^l)(\mathbf{c}^{l'}\cdot\mathbf{d}^{l'})=\sum_x[x][\mathbf{a}^l\mathbf{c}^{l'}]^x\cdot[\mathbf{b}^l\mathbf{d}^{l'}]^x, \quad (5)$$

where a shorthand notation is introduced for the coupling of two tensors with $3j$ symbols:

$$[\mathbf{a}^lS\mathbf{b}^{l'}]^x_\xi=\sum_{\lambda\lambda'}(-1)^{l-\lambda}\begin{pmatrix} l & x & l' \\ -\lambda & \xi & \lambda'\end{pmatrix}a^l_\lambda Sb^{l'}_{\lambda'}, \quad (6)$$

where there is the possibility of adding a scalar S, e.g., a Green's function, a Hamiltonian, or unity. After recoupling, we have[3]

$$F^1(\mathbf{e}_1,\mathbf{e}_2,\omega)=\sum_x\mathbf{U}^{1x}(\mathbf{e}_1,\mathbf{e}_2)\cdot\mathbf{F}^{1x}(\omega), \quad (7)$$

where the dependence on the polarization vectors is given by $\mathbf{U}^{1x}$ and the spectral line shapes are given by $\mathbf{F}^{1x}$. Note that for a dipolar transition there are three independent spectra. The recoupling allows us to study the different fundamental spectra separately. The spectra can be obtained by taking different combinations of polarization vectors. The different resonant scattering spectra are given by $x=0$, 1, and 2, where, e.g. $x=0$ is the isotropic term and $x=1$ is the $\sigma \rightarrow \pi$ scattering (note that for XMD, $x=0,1,2$ correspond to isotropic, circular dichroic, and linear dichroic spectra, respectively). The angular dependence of the scattering is now contained in the function

$$\mathbf{U}^{1x}(\mathbf{e}_1,\mathbf{e}_2)=[x][\mathbf{e}_2^*\mathbf{e}_1]^x n_{1x}, \tag{8}$$

where the normalization constants

$$n_{lx}=\begin{pmatrix} l & x & l \\ -l & 0 & l \end{pmatrix} \tag{9}$$

serve to remove the square roots of the $3j$ symbols. The square-root terms are needed for the normalization of wave functions. However, when dealing with physical quantities, it is advantegous to remove the square roots.[10] For dipolar isotropic resonant scattering, we then have $U^{10}=1$. For magnetic scattering measured in the $\sigma \rightarrow \pi$ channel, only the $x=1$ contribution remains and the angular dependence is determined by

$$U_0^{11}(\mathbf{e}_i,\mathbf{e}_f)=-\frac{i}{2}(\mathbf{e}_f^*\times\mathbf{e}_i)\cdot\hat{\mathbf{z}},$$

giving the usual $(\mathbf{k}_f\cdot\hat{\mathbf{z}})^2$ dependence.

The spectral line shapes are determined by

$$\mathbf{F}^{1x}=\langle g|[(\mathbf{T}^1)^\dagger G(\omega)\mathbf{T}^1]^x|g\rangle n_{1x}^{-1}, \tag{10}$$

where the transition operators in second quantized form follow from applying the Wigner-Eckart theorem on the spherical harmonic $\mathbf{C}^1$,

$$T_q^1=\sum_{\lambda\gamma\sigma}\langle p||\mathbf{C}^1||c\rangle(-1)^{p-\lambda}\begin{pmatrix} p & 1 & c \\ -\lambda & q & \gamma \end{pmatrix}p_{\lambda\sigma}^\dagger c_{\gamma\sigma}, \tag{11}$$

where c and $p^\dagger$ create a core hole and valence electron, respectively (for Ga and As, c and p correspond to $1s$ and $4p$, respectively). The angular- and spin-component quantum numbers are λ and $\sigma=\uparrow,\downarrow$. In the remainder, the reduced matrix element will be set to unity and spin quantum numbers are suppressed. As a result of the symmetry of the ground state, the only component of $\mathbf{F}^{1x}$ that remains is F_0^{1x}. When we write the scattering amplitude in terms of the different polarizations of the light, $\mathcal{F}_q^Q=\langle g|(T_q^Q)^\dagger G T_q^Q|g\rangle$, the energy dependence of the scattering in the $\sigma\rightarrow\pi$ channel is given by $F_0^{11}=\mathcal{F}_1^1-\mathcal{F}_{-1}^1$. Note, that for x-ray absorption this corresponds to the difference of the spectrum for left and right circularly polarized light.

Sum rules for magnetic scattering can be derived by using the fast-collision approximation,[6,9] i.e., $G(\omega)\cong\overline{G}(\omega)=(\hbar\omega-\overline{E}+i\Gamma/2)^{-1}$, where $\overline{E}$ is the average energy of the spectral line. Here, the spectral line shape is mainly determined by the Ga or As bands. The scattering amplitude can then be written in terms of valence shell ground-state expectation values[4,6,10] as

$$F_0^{1x}=\overline{G}(\omega)A_{c1p}^x\langle \underline{w}_0^x\rangle_p, \tag{12}$$

where the constant A_{c1p}^x reduces to $[p]^{-1}$ for dipole transitions $(c=p-1)$.[10] Note, that the constant A_{c1p}^x couples the core level c to the valence level p via the dipole operator (which is a tensor of order 1), leading to ground-state hole expectation values of tensors of order x. The ground-state hole expectation values are defined as

$$\langle \underline{w}_0^x\rangle_p=\sum_\lambda(-1)^{p-\lambda}\begin{pmatrix} p & x & p \\ -\lambda & 0 & \lambda \end{pmatrix}\langle p_\lambda p_\lambda^\dagger\rangle n_{px}^{-1}. \tag{13}$$

We find that the isotropic scattering amplitude $(x=0)$ is proportional to the number of holes in the p shell, $\langle \underline{w}_0^0\rangle_p=\langle n_h\rangle_p$. For $x=1$, the $\sigma\rightarrow\pi$ scattering amplitude (or circular dichroism in the case of XMD) is proportional to the normalized orbital moment, i.e., $\langle \underline{w}_0^1\rangle_p=\langle L_z\rangle_p/p$. In this approximation, the $\sigma\rightarrow\pi$ scattering amplitude is zero in the absence of an orbital moment.

To obtain a finite scattering amplitude on a nonmagnetic site, we have to go beyond the fast-collision approximation. For RXMS this leads to a finite scattering intensity. For XMD, the total intensity sum rule is exact and the inclusion of extra terms in the Green's function does not give a finite zeroth moment, i.e., integrated intensity, but leads to the presence of higher moments in the spectrum.[10] When including hybridization, we find for the lowest terms in the Green's function

$$G\cong\overline{G}+\overline{G}V^\dagger\overline{G}V\overline{G}+\overline{G}V^\dagger\overline{G}H_{\text{orbital}}\overline{G}V\overline{G}, \tag{14}$$

where we concentrate on the terms that lead to a finite $\sigma\rightarrow\pi$ scattering. The first term on the right-hand side is the fast-collision approximation and it will have a very small contribution. The other two terms are schematically given in Fig. 1. The second term describes the hopping to a valence shell on a neighboring uranium site and it can give a finite scattering amplitude if that shell has an orbital moment, for example, in UAs and UGa_3, direct hybridization of the $4p$ with the uranium $5f$ shell. It can also hop into the uranium $6d$. However, since the magnetic moment in that shell is small this will not strongly contribute to the scattering amplitude. The third term describes the hopping to a valence shell on a neighboring site with a small or zero magnetic moment where the electron interacts with a moment in a different shell on that neighboring site. In the case of UAs and UGa_3, the excited electron hops from the $4p$ shell into the uranium $6d$ shell, where it interacts with the $5f$ moment.

In the remainder, we assume that the p shell is surrounded by six nearest neighbors in a cubic environment and the magnetic moment is parallel to the [001] crystal axis. This situation corresponds to that of UAs. We will now formally prove that angular momentum can only be transferred along the axis of the magnetic moment, i.e. the z axis. The hybridization is then given by

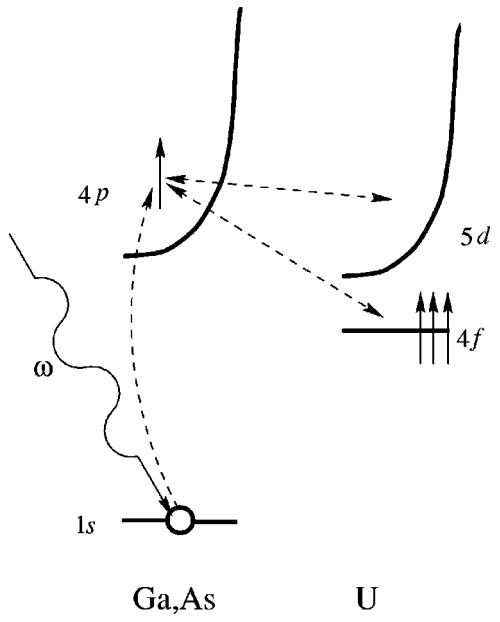

FIG. 1. Schematic picture of the different ways an excited electron on the Ga or As atom can interact with the uranium moment. First, it can directly hop into the polarized $6d$ or $5f$ shell and ''probe'' the moment. Secondly, it can hop into the $6d$ shell and interact with the $5f$ moment.

$$V=\sum_{\mathbf{R}}\sum_{\lambda\tilde{\lambda}\lambda'\tilde{\lambda}'} D^{l*}_{\lambda',\tilde{\lambda}'}(\mathbf{R})V_{pl\mathbf{R}}D^{p}_{\tilde{\lambda},\lambda}(\mathbf{R}), \tag{15}$$

where $D^{l}_{\tilde{\lambda},\lambda}(\mathbf{R})$ are rotation matrices[11] that transform the orbitals to a new coordinate system with its z axis pointing towards the nearest neighbor at position $\mathbf{R}$.

The hybridization along the new z axis is diagonal

$$V_{pl\mathbf{R}}=V_{pl\sigma}l^{\dagger}_{\mathbf{R}0}p_0+V_{pl\pi}(l^{\dagger}_{\mathbf{R}1}p_1+l^{\dagger}_{\mathbf{R},-1}p_{-1}), \tag{16}$$

where $l^{\dagger}_{\mathbf{R}\lambda}$ creates an electron at the neighboring uranium site $\mathbf{R}$ with angular quantum number λ, and $V_{pl\sigma}$ and $V_{pl\pi}$ are the hybridization matrix elements between p and l orbitals with σ and π overlap, respectively.[12] We can now couple the D^{p} rotation matrices from the V and $V^{\dagger}$ with each other and make use of the relation

$$\sum_{\lambda\lambda'}(-1)^{p-\lambda'}\begin{pmatrix} p & x & p \\ -\lambda' & 0 & \lambda \end{pmatrix}D^{p}_{\lambda',\tilde{\lambda}'}(\mathbf{R})D^{p}_{\lambda,\tilde{\lambda}}(\mathbf{R})$$
$$=(-1)^{p-\tilde{\lambda}'}\begin{pmatrix} p & x & p \\ -\tilde{\lambda}' & \tilde{\lambda}'-\tilde{\lambda} & \tilde{\lambda} \end{pmatrix}D^{p}_{0,\tilde{\lambda}'-\tilde{\lambda}}(\mathbf{R}). \tag{17}$$

For σ hybridization, we obtain $n_{pxp}C^{x}_{0}(\theta)$ with θ the angle between $\mathbf{R}$ and the z axis, where we have made use of the relation between the rotation matrices and the spherical harmonics.[11] The factor n_{xyz} is given by[10]

$$n_{xyz}=\begin{pmatrix} x & y & z \\ 0 & 0 & 0 \end{pmatrix}. \tag{18}$$

The coefficients n_{xyz} are zero when $x+y+z$ is odd. For $x=1$, n_{pxp} is zero and the σ hybridization gives no contribution to the scattering amplitude. For π hybridization with $x=1$, one has $n_{p1}C^{1}_{0}(\theta)=1/[p]\cos\theta$, which is zero for $\theta=\pi/2$. Therefore, for $x=1$ a nonzero scattering amplitude is only obtained for the π hybridization matrix elements along the z axis. No angular momentum is transferred in the xy plane if the moments are along the z axis since the angular momentum information is lost in the hybridization process which involves a combination of $\lambda=\pm1$ orbitals. However, along the z axis only orbitals with equal λ couple with each other and angular momentum information can be transferred. Note that, since we are looking at the K edge, the scattering is only sensitive to angular momentum and not to spin.

In the perturbation series approach in Eq. (14), we can simply add the contributions from the neighboring sites. For our purposes, it is convenient to write the hybridization along the z axis as a Clebsch-Gordan coefficient. For our purposes, it is convenient to write the hybridization along the z axis as a $3j$ symbol; for $\kappa=l$ one has

$$V_{plz}=\sqrt{2[l]}V_{pl\pi}\sum_{\lambda}(-1)^{l-\lambda}\begin{pmatrix} l & \kappa & p \\ -\lambda & 0 & \lambda \end{pmatrix}l^{\dagger}_{\lambda}p_{\lambda}. \tag{19}$$

The scattering amplitude can now be written as a product of $3j$ symbols of the hybridization and the dipole matrix elements. This can be simplified by the use of spherical tensor algebra.[11] For the second term on the right-hand side of Eq. (14), we find

$$F^{1x}_{0}(\omega)=V^{2}_{pl\pi}\overline{G}^{3}(\omega)\langle \underline{W}_{l}\rangle \tag{20}$$

with the operator

$$\underline{W}_{l}=\sum_{yz}\mathcal{A}^{xyz}_{c1p\kappa l}\langle \underline{w}^{z}_{0}\rangle_{l}. \tag{21}$$

The coefficients are given by

$$\mathcal{A}^{xyz}_{c1p\kappa l}=\frac{2[lyz]}{[p]}\begin{Bmatrix} p & x & p \\ \kappa & y & \kappa \\ l & z & l \end{Bmatrix}n_{\kappa\kappa y}n_{xyz}n_{lz}n^{-1}_{1x}, \tag{22}$$

where we have taken dipolar transitions ($c=p-1$). This result should be compared with the sum rule for RXMS in the fast-collision approximation, $F^{1x}_{0}=\overline{G}(\omega)A^{x}_{c1p}\langle \underline{w}^{x}_{0}\rangle_{p}$. We see here that the constant $\mathcal{A}^{xyz}_{c1p\kappa l}$ couples the core level c to the valence level p, which is coupled via κ to the valence shell l on a neighboring site. The scattering amplitude is now expressed in ground-state expectation values of tensors of order z in shell l. Note, that the order of the tensor is no longer x, but is changed by the hybridization into z. The normalization constants n_{xyz} are zero when $x+y+z$ is odd. The presence of $n_{\kappa\kappa y}$ ensures that y is even, and therefore that z is odd/even when x is odd/even. When evaluating the constants $\mathcal{A}^{xyz}_{c1p\kappa l}$, we find

$$\langle \underline{W}_{d}\rangle=\tfrac{2}{15}(\langle \underline{w}^{1}_{0}\rangle_{d}-\langle \underline{w}^{3}_{0}\rangle_{d}), \tag{23}$$

$$\langle \underline{W}_{f}\rangle=\tfrac{1}{14}(\langle \underline{w}^{1}_{0}\rangle_{f}-\tfrac{14}{9}\langle \underline{w}^{3}_{0}\rangle_{f}+\tfrac{5}{9}\langle \underline{w}^{5}_{0}\rangle_{f}) \tag{24}$$

for $l=d$ and f, respectively. We see that the scattering amplitude is not only proportional to the $\langle w_0^1\rangle_l=\langle L_z\rangle_l/l$, but also to higher-order moments of the electron distribution on the neighboring site. For example, $\underline{w}_0^3\sim(3\mathbf{L}^2-5L_z^2-1)L_z$.[13]

One can also look at the combination of operators in a different way. Note that $\sigma\rightarrow\pi$ scattering on Ga or As gives $\mathcal{F}_1^1-\mathcal{F}_{-1}^1$. The effect of the hybridization is to make a transition to uranium $5f$ or $6d$ orbitals without changing the angular momentum. The combination of a dipole plus the hybridization with the $6d$ shell creates an effective quadrupolar transition to a neighboring site whose spectrum for $\sigma\rightarrow\pi$ scattering ($x=1$) is given by $\mathcal{F}_1^2-\mathcal{F}_{-1}^2$. However, for normal quadrupole magnetic scattering, the odd F^{2x} terms are given by

$$F_0^{21}=\mathcal{F}_2^2+\frac{1}{2}\mathcal{F}_1^2-\frac{1}{2}\mathcal{F}_{-1}^2-\mathcal{F}_{-2}^2, \tag{25}$$

$$F_0^{23}=\mathcal{F}_2^2-2\mathcal{F}_1^2+2\mathcal{F}_{-1}^2-\mathcal{F}_{-2}^2. \tag{26}$$

The total scattering amplitude is an angular-dependent combination of F^{21} and F^{23}. We can write $\mathcal{F}_1^2-\mathcal{F}_{-1}^2=\frac{2}{5}(F_0^{21}-F_0^{23})$. Since the sum rule for the quadrupolar scattering amplitude into a d shell shows that $F^{2x}\sim\langle\underline{w}_0^x\rangle_d$, we can directly see that the scattering amplitude is proportional to $\langle\underline{w}_0^1\rangle_d-\langle\underline{w}_0^3\rangle_d$. The same argument works for hybridization with a f shell, but here we need to consider an effective octupolar transition. Another way to see effective higher-order transitions created is by noting that for Q polar $\sigma\rightarrow\pi$ scattering the maximum obtainable rank of a tensor is $2Q-1$. Therefore, for dipolar scattering we can only probe tensors of order one (e.g., $w^1\sim L_z$ or S_z). To measure higher moments of the charge distribution one needs higher-order transitions. Note that this effective higher-order scattering process only relates to the electronic part F_0^{1x}, and the angular part U_0^{1x} still shows the typical dipolar dependence, as observed by Mannix *et al.*[8]

For the $5f^3$ and $5f^2$ configurations of uranium, $\langle\underline{W}_f\rangle$ is 0.267 and 0.077, respectively. The small value for two electrons, $5f^2$, can be understood from the small occupation in the ground state of the angular quantum numbers ±1. For two holes ($5f^{12}$), this ground-state expectation value is zero. The small value for $5f^2$ is a result of the coupling of L and S to $|L-S|$ instead of $L+S$.

Let us now turn our attention to the third term on the right-hand side of Eq. (14). This describes the situation where the excited electron hops to a neighboring uranium $6d$ orbital and interacts with the $5f$ shell. For $x=1$, a finite scattering amplitude is obtained from the exchange term in the df Coulomb interaction (the direct term does not contribute):

$$H_{\text{orbital}}=\sum_{k\lambda\varphi\lambda'\varphi'}\sum_{\sigma\sigma'}\delta_{\varphi'-\lambda',\varphi-\lambda}c^k(f\varphi',d\lambda')c^k(f\varphi,d\lambda)\times G^k f^\dagger_{\varphi'\sigma}d^\dagger_{\lambda'\sigma'}f_{\varphi\sigma'}d_{\lambda\sigma}, \tag{27}$$

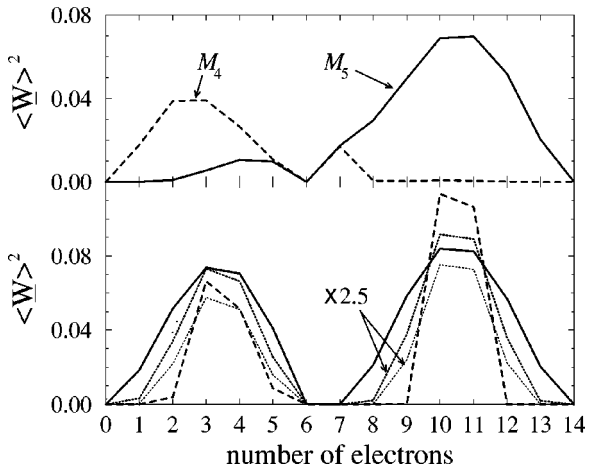

FIG. 2. The lower part shows the ground-state expectation value squared of $\underline{W}_f$ (dashed line) and $\underline{W}_f^G$ (dotted line) for different numbers of f electrons. The expressions are given in the text. For the exchange integrals, a typical relative strength of $G^1:G^3:G^5=1:0.6:0.4$ was taken. The thin dotted line shows the contribution of G^1. Notice the difference in behavior from the operator $\langle\underline{W}\rangle^2$ with $\underline{W}=\frac{1}{7}\underline{w}_0^1=\frac{1}{21}\langle L_z\rangle$ (solid line). The upper part shows the trend along the f series for scattering at the $M_{4,5}$ edges, with $\underline{W}=\frac{1}{35}(3\underline{w}^1+\frac{4}{3}S_z+4T_z),\frac{1}{35}(2\underline{w}^1-\frac{4}{3}S_z-4T_z)$ for the M_5 and M_4 edges, respectively (Ref. 5).

where G^k are the Slater integrals. The coefficients c^k are related to $3j$ symbols.[16] Solving the scattering amplitude for this interaction gives

$$F_0^{1x}(\omega)=V_{pl\pi}^2\overline{G^4}(\omega)\langle\underline{W}_f^G\rangle, \tag{28}$$

where the operator is given by

$$\langle\underline{W}_f^G\rangle=\sum_{kyz}\mathcal{A}^{xyz}_{c1p\kappa d}\mathcal{B}^z_{dkf}\langle\underline{w}_0^z\rangle_f, \tag{29}$$

where $\mathcal{A}^{xyz}_{c1p\kappa d}$, see Eq. (22), describes the coupling of the core hole to a d orbital on a neigboring site and

$$\mathcal{B}^z_{dkf}=n^2_{dkf}[df]\begin{Bmatrix}d & z & d\\ f & k & f\end{Bmatrix}G^k n_{dz}^{-1}n_{fz} \tag{30}$$

gives the coupling of the d orbital to the magnetic moment on the f shell via the Coulomb interaction. Note that the ground-state expectation values are now for the f shell, although the Coulomb interaction, being scalar, does not change the rank z of the operator.

Evaluating the coefficients gives

$$\langle\underline{W}_f^G\rangle=-\tfrac{2}{35}\{(G^1+\tfrac{1}{6}G^3+\tfrac{25}{66}G^5)\langle\underline{w}_0^1\rangle_f+(-G^1+\tfrac{8}{27}G^3+\tfrac{25}{297}G^5)\langle\underline{w}_0^3\rangle_f\}. \tag{31}$$

For the resonant scattering the G^1 term is dominant, see Fig. 2. We find that the operator dependence w^1-w^3 is the same as that for hybridization with a d shell. This can be understood from the fact that the angular part of the exchange Coulomb interaction is equal to an isotropic dipolar scattering process between the d and the f shell.[14]

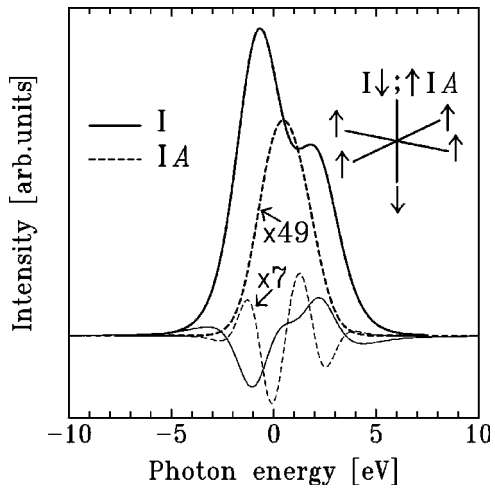

FIG. 3. The RMXS (thick lines) and magnetic circular dichroism (thin lines) for dipolar excitation at the *K* edge. The *p* orbital is octahedrally surrounded by six *d* shells which have spin and orbital polarization, see the inset. Spectra are calculated for the type-I (solid line) and type-I*A* (dashed line) magnetic structures of UAs. The spins in the inset indicate schematically the sign of the orbital and spin polarization.

The trend along the *f* series is given in Fig. 2. Note that the behavior is different from $\langle L_z \rangle^2$. Differences are especially pronounced when the *f* shell is almost full or empty, or close to half filling. The behavior differs strongly from dipolar scattering at the *M* edges, where also spin-dependent operators (S_z and T_z) contribute to the scattering amplitude.

The ratio of the integrated scattering amplitudes coming from direct hybridization with the polarized *f* and from interaction with the *f* shell via the *d* shell is $\frac{10}{3} g(G^1/\Gamma)^2 (V_{pd\pi}/V_{pf\pi})^4$, where we restrict ourselves to the largest contribution coming from the G^1 term. The values for *g* of 2.77 and 0.33 for $5f^2$ and $5f^3$, respectively, follow from the ground-state expectation values of $\underline{w}_0^z$ for the different number of *f* electrons. Considering also that $V_{pd\pi} > V_{pf\pi}$, we find that, for uranium compounds, the contribution from Eq. (31) is the largest.

In an independent particle framework, the interaction between the *d* and *f* electrons is usually simplified to an orbital polarization on the *d* shell, $H_{\text{orbital}} = \Delta_d \Sigma_\lambda \lambda d_\lambda^\dagger d_\lambda$. In the limit that the occupation of the *d* orbital can be neglected, the scattering amplitude is directly proportional to the magnitude of the orbital polarization,

$$F_0^{11} = -\frac{10}{3} V_{pd\pi}^2 \overline{G}^4(\omega) \Delta_d . \tag{32}$$

Figure 3 shows a numerical example on a small cluster of the RXMS and circular dichroism for a $1s \rightarrow np$ dipolar transition using orbital polarization. The *p* shell is octahedrally surrounded by six *d* shells that have orbital and spin polarization. The parameters are $V_{pd\pi} = -0.5$ and $V_{pd\sigma} = 1.0$ eV, a charge transfer energy $\varepsilon_d - \varepsilon_p = 1.0$ eV, an orbital polarization $\Delta_d = 0.5$ eV, and a spin polarization $\Delta_s = 1.0$ eV. Band effects are partially included in the lifetime broadening of $\Gamma = 5.0$ eV. The spectrum has been obtained by exact diagonalization. In the type-I structure ($T_N \sim 126$ K), UAs exhibits ferromagnetic planes which are stacked antiferromagnetically[15] in the sequence $+-+-$. We see a finite scattering amplitude caused by a difference in resonance energies for $\lambda = +1$ and -1. Since we are dealing with scattering at the *K* edge, spin polarization alone is not sufficient to cause a finite scattering amplitude. Sensitivity to spin polarization would be present for excitations at a spin-orbit split edge. The integrated intensity of the circular dichroism is, as one would expect, zero. The spectrum shows $\text{Im}[\overline{G}^4(\omega)]$ behavior with some extra structure resulting from the difference between the spin-up and spin-down spectra. Note, that this structure has the same magnetic and chemical unit cell and will therefore overlap with the normal charge scattering.

RXMS was observed in the type-I*A* structure (found below $T = 63.5$ K), where the stacking of ferromagnetic planes is $++--$, making the magnetic unit cell twice as large as the chemical one. Although the orbital polarization at the sites at $\pm R\hat{\mathbf{z}}$ is opposite, it is still possible to obtain a finite scattering amplitude since their contributions are not entirely equivalent, see the dashed lines in Fig. 3. The circular dichroism spectrum has now more structure. To explain this, the spin polarization is crucial. Without spin polarization, the sites at $\pm R\hat{\mathbf{z}}$ would give equal $\overline{G}^4$-type contributions but of opposite sign. However, the contribution from the site with the spin parallel to that of the excited electron has a somewhat smaller $\overline{E}$ by the spin polarization. This gives $\overline{G}^5$-like shape. In addition to that, the spin-up and spin-down channels are different as a result of the ferromagnetic coupling in the planes, resulting in a spectral line shape that has a $\overline{G}^6$-type line shape.

Mannix *et al.*[8] give (for the absolute intensities) over 10^5 counts/s (at 200-mA synchrotron current) at the U $M_{4,5}$ edges and up to 8×10^4 counts/s for the scattering at the As *K* edges. The integrated intensity for scattering at the $M_{4,5}$ edge is proportional to $P_{\text{U}}^4 2\pi/\Gamma$, where we have used the fact that the integration over $|\overline{G}(\omega)|^2$ is $2\pi/\Gamma$. P_{U} is the reduced matrix element for uranium. Using Eq. (28), we find that the integrated intensity of the scattering at the As *K* edge is proportional to $a_{\text{As/Ga}}^4 (G^1 V_{pd\pi}^2 P_{\text{As/Ga}}^2)^2 (2\pi/\Gamma)^4$. Estimates of the absolute intensities strongly depend on the parameters. The constant $a_{\text{As/Ga}}$ also varies from two to six depending on the number of Ga/As ions in the system and it could be somewhat reduced as a result of the alignment of the spins along the *z* axis. A calculation in the atomic limit using Cowan's programs[16] gives $P_{\text{U}}/P_{\text{As}} = 0.045/0.0066 \cong 7$ and $G^1 = 2.4$ eV. Values for Ga are very similar. The effective operator for the As *K* edge is about twice that of the U M_4 edge. Using $V_{pd\pi} \cong 0.5 - 0.7$ eV and $\Gamma \cong 4$ eV, we obtain that the scattering intensity at the As *K* edge is roughly 10–100 times smaller than the intensity at the U $M_{4,5}$ edge. This is in agreement with experimental estimates of the scattering intensities by Mannix *et al.*[8] The intensity of UAs is estimated to be smaller than that of UGa_3.

In conclusion, we have studied the phenomena of resonant magnetic x-ray scattering at the *K* edge of nonmagnetic

ions. Effectively, the excited electron probes the different moments of the orbital polarization at the neighboring sites. The results can be written as effective quadrupolar and octupolar transitions from the Ga/As $1s$ level into the U $5f$ and $6d$ orbitals, respectively. Note, that the absorption process is still dipolar and one therefore observes a dipolar angular dependence of the scattering amplitude. In addition, the resonant process is essential in obtaining a finite scattering amplitude, since it is the excited electron that ''probes'' the neighboring sites. This explains the strong enhancement with respect to the nonresonant scattering amplitude. More experimental work needs to be done to assess the trends of the scattering for different actinide (or rare-earth) ions. For transition metals, where the orbital polarization is small, it would be interesting to study scattering at spin-orbit split edges, where the excited electron can also probe spin polarization.

This work was supported by the State of Illinois under HECA.

[1] G. Schütz, W. Wagner, W. Wilhelm, P. Kienle, R. Zeller, R. Frahm, and G. Materlik, Phys. Rev. Lett. **58**, 737 (1987).
[2] D. Gibbs, D. R. Harshman, E. D. Isaacs, D. B. McWhan, D. Mills, and C. Vettier, Phys. Rev. Lett. **61**, 1241 (1988).
[3] J. P. Hannon, G. T. Trammell, M. Blume, and D. Gibbs, Phys. Rev. Lett. **61**, 1245 (1988).
[4] B. T. Thole, P. Carra, F. Sette, and G. van der Laan, Phys. Rev. Lett. **68**, 1943 (1992).
[5] P. Carra, B. T. Thole, M. Altarelli, and X. Wang, Phys. Rev. Lett. **70**, 694 (1993).
[6] J. Luo, G. T. Trammell, and J. P. Hannon, Phys. Rev. Lett. **71**, 287 (1993).
[7] M. van Veenendaal, J. B. Goedkoop, and B. T. Thole, Phys. Rev. Lett. **78**, 1162 (1997).
[8] D. Mannix, A. Stunault, N. Bernhoeft, L. Paolasini, G. H. Lander, C. Vettier, F. de Bergevin, D. Kacrozowski, and A. Czopnik, Phys. Rev. Lett. **86**, 4128 (2001).
[9] P. Carra, M. Fabrizio, and B. T. Thole, Phys. Rev. Lett. **74**, 3700 (1995).
[10] B. T. Thole, G. van der Laan, and M. Fabrizio, Phys. Rev. B **50**, 11 466 (1994); **50**, 11 474 (1994).
[11] M. E. Rose, *Elementary Theory of Angular Momentum* (Wiley, New York, 1957).
[12] J. C. Slater and G. F. Koster, Phys. Rev. **94**, 1498 (1954).
[13] P. Carra, H. König, B. T. Thole, and M. Altarelli, Physica B **192**, 182 (1993).
[14] M. van Veenendaal, J. B. Goedkoop, and B. T. Thole, Phys. Rev. Lett. **77**, 1508 (1996).
[15] S. K. Sinha, G. K. Lander, S. M. Shapiro, and O. Vogt, Phys. Rev. B **23**, 4556 (1981).
[16] R. D. Cowan, *The Theory of Atomic Spectra* (University of California, Berkeley, 1981).